Conductivity of the Si(111)7×7 dangling-bond state

Marie D'angelo,* Keiko Takase, Nobuhiro Miyata, Toru Hirahara, and Shuji Hasegawa
Department of Physics, School of Science, The University of Tokyo, 7-3-1 Hongo, Bunkyo-ku, Tokyo 113-0033, Japan

Akinori Nishide, Manami Ogawa, and Iwao Matsuda†
Synchrotron Radiation Laboratory, Institute for Solid State Physics, The University of Tokyo, 5-1-5 Kashiwanoha, Kashiwa 277-8581, Japan

(Received 3 March 2008; revised manuscript received 6 November 2008; published 20 January 2009)

Conductivity of the metallic dangling-bond state of adatoms on Si(111)7×7 clean surface was determined through passivation of the only electrical channel by ~0.1 monolayer Na adsorption. Through systematic measurements of electron transport and photoemission spectroscopy during the Na deposition, Si(111)7×7 was found to exhibit a metal-to-insulator transition. The decrease in conductivity through the transition, which is attributed to the conductivity of the dangling-bond state, was 2–4 $\mu\Omega^{-1}\,\square^{-1}$. The value is smaller than the two-dimensional Ioffe-Regel limit and the mean-free path is too short to apply the Boltzmann picture.

DOI: 10.1103/PhysRevB.79.035318 PACS number(s): 73.25.+i, 73.20.−r, 79.60.Bm

I. INTRODUCTION

The topmost layer (surface superstructure) of a semiconductor crystal is an intriguing playground to study low-dimensional transport phenomena at the atomic scale.[1,2] However, it has been experimentally difficult to measure conductivity of *only* the surface atomic layer and to eliminate contributions from the subsurface (bulk and space-charge) layers. The Si(111)7×7 clean surface has been one of the most famous surface superstructures that has been challenged to reveal its electron-transport phenomena by varieties of experimental techniques. The surface is metallic according to photoemission spectroscopy, in contrast to the semiconductor nature of the substrate, and the atomic structure is described by the dimer–adatom-stacking (DAS) fault model. At each adatom, there is a partially filled dangling-bond toward vacuum [Fig. 1(a)].[3–6] Such a surface state is located in the band gap of the bulk bands, so that the surface state is electronically decoupled from the substrate bulk. Electron transport through the metallic state (surface-state conductivity) [Fig. 1(a)] has been the central issue among researchers for the past two decades, but any consensus has not been reached yet. Analysis of the electron energy-loss spectroscopy results[7] estimated that the ac conductivity was in the order of $\mu S/\square$ (10^{-6} $\Omega^{-1}/\square$) and a point contact of scanning tunneling microscope (STM) tip[8] detected a possible electrical conductivity of $\mu S/\square$ at the surface. Later, dc conductivity measurements were conducted by four-terminal methods with various probe spacings.[9–11] These researches found that the measured conductivities were comparable to those of the Si substrates (bulk and space-charge layers) although they also deduced that the surface-state conductivity was in the $\mu S/\square$ range. Some groups have fabricated artificial insulators by using semiconductor-on-insulator (SOI) wafers[12] or trenches scratched by a STM tip on a surface[13] to acquire enough surface sensitivity. However, these experiments reported quite higher (~100 $\mu S/\square$) and lower ($\sim 10^{-3}$ $\mu S/\square$) conductivities, respectively, than other transport reports. Figure 1(b) summarizes the sheet conductivities of the Si(111)7×7 surface reported by various transport measurement techniques together with their brief explanation.

Measuring changes in conductivity caused by surface passivations or surface phase transitions has been one of the powerful methods to determine the surface conductivity since it intrinsically eliminates the contribution of bulk layers from the experimental results completely. The methods using the surface phase transition by metal adsorption have succeeded in measuring longitudinal and transverse (Hall) resistivities of various 2D metallic monolayers on Si(111).[9,14,15] Passivations of semiconductor clean surfaces by active gas, i.e., oxygen, have been conventionally used to determine surface conductivity.[8,9,12,16] Since, however, sur-

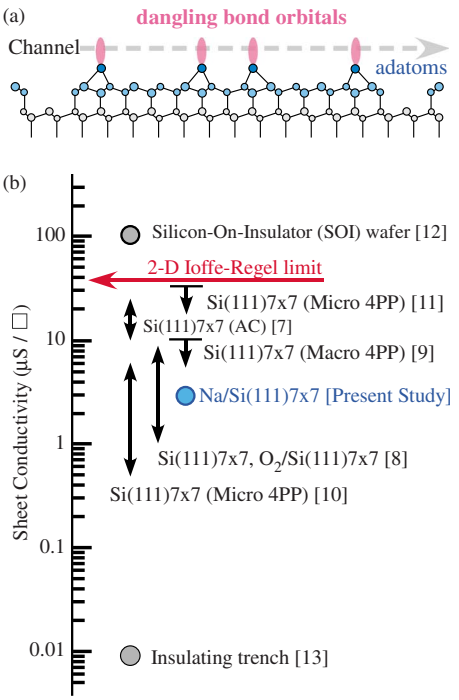

FIG. 1. (Color online) (a) Structure model of Si(111)7×7 with an electric channel of the dangling-bond state of adatoms. (b) A summary of the Si(111)7×7 sheet conductivity measured at room temperature by various experiments. The two-dimensional (2D) Ioffe-Regel limit is also indicated.

face band bendings are sensitive to conditions of surfaces, the measured conductivity changes contain contributions from both of the surface topmost and space-charge layers. In the case of Si(111)7×7, the surface oxidization is complex and, therefore, the induced change in band bending is also complicated. The previous transport experiments of Si(111)7×7 with oxygen exposure have detected change of surface conductivities but their results were not reproducible among the literature.[8,12,16,17] As a consequence, reported conductivities of Si(111)7×7 have, so far, scattered in the 10^{-3}–10^{2} μS/□ range [Fig. 1(b)].

In the present research, we have adopted a different approach to this issue of electron transport in Si(111)7×7. Instead of oxygen adsorption, we put very small amount of sodium on the surface and *systematically* studied the evolution of electron transport and electronic structure. By Na adsorption of ~0.1 monolayer (ML), the metallic surface-state bands disappeared and the surface band bending shifted about 60 meV toward the Fermi level. Through this metal-to-insulator transition, reduction in the conductivity was measured by four-terminal methods with macroscopic and microscopic probe spacings, giving the similar values. The decreased conductivity of 2–4 μS/□ was much larger than the one estimated for the subsurface layers (space-charge layers) of a nondoped Si wafer. Therefore, the measured change corresponded to the conductivity of an electrical channel of only the metallic dangling-bond state shown in Fig. 1(a). Despite the various kinds of the band structures of Si(111)7×7 reported previously, the measured transport parameters do not agree with the ones estimated through either the Drude model or the Boltzmann equation. The electron transport of a long-period surface phase of Si(111)7×7 raises a new intriguing issue in two-dimensional transport phenomena.

II. EXPERIMENTS

The electronic structure was studied by angle-resolved photoemission spectroscopy with unpolarized He $I\alpha$ radiation and an electron spectrometer (Scienta SES-100) with an energy resolution of about 35 meV.[14] Electrical conductivity was measured *in situ* in two separate chambers by four-terminal methods with linearly aligned four probes of macroscopic and microscopic probe spacings.[9,10] Details of the two experimental systems are described in Sec. III. The electrical resistance R was determined from the slope of linear current-voltage curves that were obtained by sweeping the current I flowing between the outer pair of probes and measuring the voltage drop ΔV between the inner pair of probes, $R=d(\Delta V)/dI$. A clean Si(111)7×7 surface was prepared on an n-type (1–10 Ω cm) or a p-type (3900–6400 Ω cm) Si(111) wafer by a cycle of resistive heat treatments. The high-resistivity p-type Si sample corresponds typically to a nondoped one. The quality and cleanliness of Si(111)7×7 was ascertained *in situ* by a sharp pattern of reflection high-energy electron diffraction and strong surface-state signals in the valence-band photoemission spectra. Sodium atoms were evaporated by using commercial SAES-getter sources which were thoroughly outgassed to minimize any impurity effects.

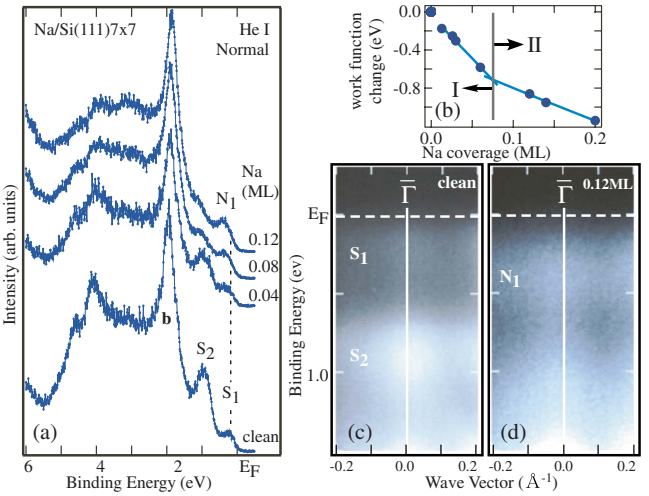

FIG. 2. (Color online) (a) Na-coverage dependence of normal-emission photoelectron spectra. (b) Work-function change with Na coverage, measured by the cutoff in photoemission spectra. Two stages of the initial Na adsorption (less than 0.2 ML) are classified at ~0.08 ML. [(c) and (d)] Band dispersion diagrams at the $\bar{\Gamma}$ point for (c) clean Si(111)7×7 and (d) 0.12 ML Na-covered surfaces.

The Na coverage was calibrated by work-function change and appearance of various surface ordered phases on Si(111).[14,18–21]

III. RESULTS AND DISCUSSION

Figure 2(a) shows a series of normal photoemission spectra with different Na coverage. The S_1 state at Fermi level (E_F) and S_2 state at a binding energy (E_b) of ~1 eV correspond to the dangling-bond states of adatoms and rest atoms on Si(111)7×7, respectively, while the **b** state at E_b ~2 eV is assigned to the bulk Si state.[3,5,22] As the Na atoms adsorbed up to 0.12 ML, S_1 and S_2 peaks disappeared and the N_1 state appeared instead at E_b~0.3 eV. The spectral change was found at the first (**I**) stage (less than 0.08 ML) of the Na growth classified by the reported discontinuous change in work function.[18,19] According to the previous STM report, 2D Na gas was formed without destroying the 7×7 surface at this coverage.[18] As shown in Fig. 2(b), we have also traced the same work-function change as in the previous reports.[18,19] Figures 2(c) and 2(d) show experimental band diagrams at the $\bar{\Gamma}$ point for (c) clean and (d) 0.12 ML Na-covered surfaces. In contrast to observation of a metallic surface (S_1) in Fig. 2(c), there is only an insulating state (N_1) in Fig. 2(d). Therefore, at stage **I** of adsorption, the surface exhibits the Na-induced metal-to-insulator transition, which was also confirmed by the previous photoemission spectroscopy study.[19] On the other hand, the present high-resolution photoemission spectroscopy found that energy position of the bulk state **b** shifted about 60 meV toward E_F through the **I** stage [Fig. 2(a)]. The photoemission results in Fig. 2 were measured with the n-type (1–10 Ω cm) Si wafer. The same band-bending change was also confirmed by photoemission spectroscopy for the p-type (3900–6400 Ω cm). It is noted that such independence of band-bending change by doping

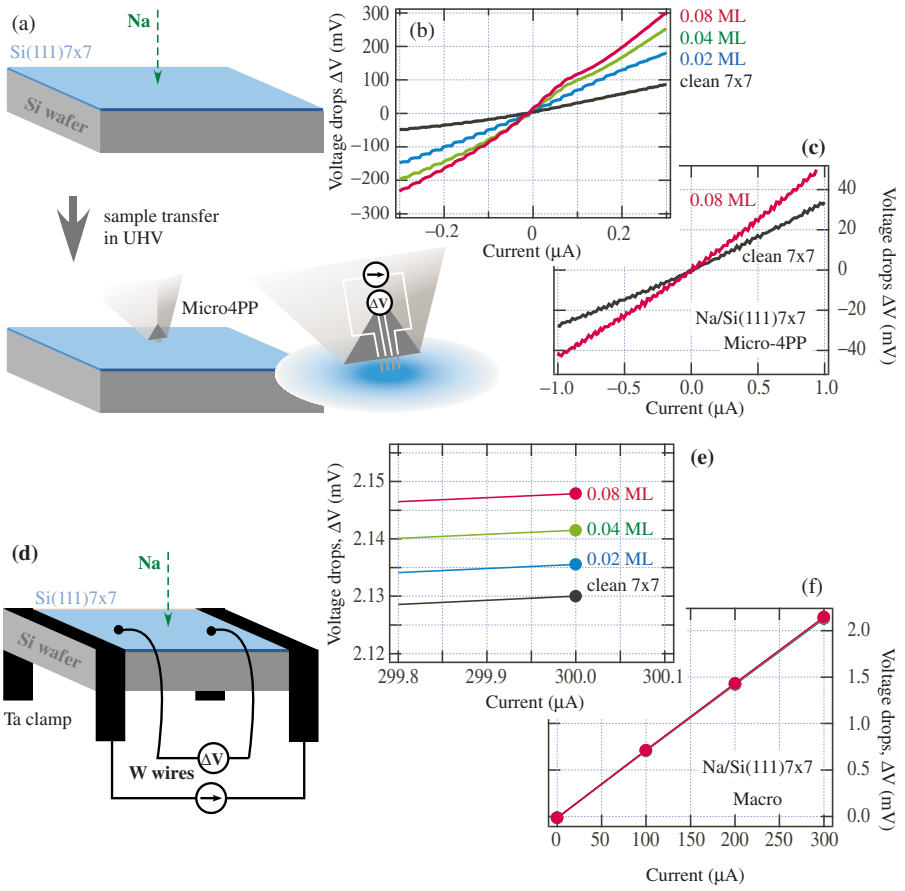

FIG. 3. (Color online) Schematic pictures for conductivity measurements of Na/Si(111)7×7 by (a) microscopic and (d) macroscopic four-terminal methods. (a) Na was deposited on a clean surface *prior to* conductivity measurements with microscopic four-point probe (4PP) (micro-4PP) of (d) 20-μm probe spacing while Na was deposited during the measurements for the macroscopic arrangement. [(b) and (c)] Current-voltage curves with different Na coverage taken by (b) the microscopic 4PP on the *n*-type (1–10 Ω m) and (c) on the *p*-type (3900–6400 Ω m) Si wafers. [(e) and (f)] Current-voltage curves measured on the *p*-type wafer by the macroscopic (macro) case. (e) shows details of voltage drops measured at current of 300 μA.

levels of bulk semiconductors is known as "Fermi-level pinning."[23] These electronic evidences indicate that ~0.1 ML 2D Na gas completely eliminates metallic surface states of Si(111)7×7 and makes band-bending change of ~60 meV beneath the surface. Therefore, in order to find a proper relation between the change in electrical resistance and elimination of the metallic dangling-bond state at the **I** stage, conductivity changes in space-charge layers need to be estimated for the sample Si wafers.

In the present research, transport measurements were performed at room temperature by four-terminal method in two different ultrahigh-vacuum (UHV) systems. One was composed of separate preparation and measurement chambers. As shown in Fig. 3(a), prior to conductivity measurements, Na atoms were deposited on Si(111)7×7 at room temperature in a preparation chamber. Then, the sample was transferred under UHV condition to the measurement chamber in which a monolithic micro-four-point probe (probe spacing: 20 μm) was set. The microscopic method has high surface sensitivity and it has succeeded in measuring conductivities of one-dimensional and two-dimensional metallic surface structures.[11,24–27] As shown in Figs. 3(b) and 3(c), slopes of linear current-voltage curves obviously become larger with Na coverage. Namely, surface resistance (conductance) increases (decreases) by Na deposition on the clean Si(111)7×7 surface.

The other transport measurement system was a single UHV chamber equipped with four probes of macroscopic (~10 mm) spacing on a sample surface.[2,11] In contrast to the microscopic method, the distance between the probes was long enough to enable conductivity measurement *during* the Na deposition as shown in Fig. 3(d). Since the macroscopic measurement is sensitive to the bulk conduction, the current-voltage curves show little dependence to the Na coverage, as shown in Fig. 3(f). However, by a close look of voltage drops at current of 300 μA, one can recognize systematic change with Na coverage: the voltage drop becomes large with Na deposition [Fig. 3(e)]. This also indicates an increase in surface resistance by Na adsorption on the clean Si(111) surface.

Figure 4 shows the change in conductivity by Na deposition on the Si(111)7×7 surface. For the microscopic four-point probe method, the change in sheet conductivity $\Delta\sigma_{\text{micro}}$ is expressed as[1]

$$\Delta\sigma_{\text{micro}} = \sigma_{\text{micro}} - \sigma_{\text{micro0}}, \tag{1}$$

$$= \frac{\ln 2}{\pi}\left(\frac{1}{R_{\text{micro}}} - \frac{1}{R_{\text{micro0}}}\right), \tag{2}$$

where σ_{micro0} (R_{micro0}) is the conductivity (resistance) before the Na deposition. As shown in Fig. 4, the average conductivity decreases and, by the completion of the Na growth stage of **I**, σ_{micro} has reduced by about 3 μS/□.

While the sample size was infinitively larger than the probe spacing in the microscopic 4PP experiment, it was comparable to the probe spacing in the macroscopic arrangement. The difference leads to distinctive solutions of the

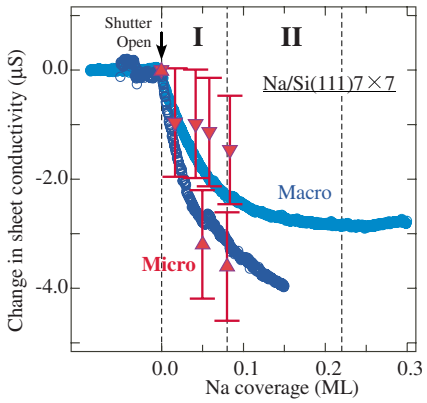

FIG. 4. (Color online) Change in conductivity by Na deposition on Si(111)7×7 measured by four-point probe method with the macroscopic and microscopic (micro)probe spacings. The changes were referred from the conductivity of initial Si(111)7×7 measured by individual methods. An arrow in the figure indicates opening of the Na source shutter in the macroexperiment. Typical curves of continuously measured conductivity by the macromethod are plotted as blue circles (p type, 3900–6400 Ω m), while data points of average conductivity values taken stepwisely by the micromethod are shown by red triangles pointing up (p type, 3900–6400 Ω m) or down (n type, 1–10 Ω m). The error bars are also indicated.

Poisson equation. The electrical resistance (R_{macro}), measured by the macroscopic four-terminal method, is converted to the change in sheet conductivity $\Delta\sigma_{\mathrm{macro}}$ through the relation[1,2]

$$\Delta\sigma_{\mathrm{macro}} = \sigma_{\mathrm{macro}} - \sigma_{\mathrm{macro0}}, \tag{3}$$

$$= \frac{L}{W}\left(\frac{1}{R_{\mathrm{macro}}} - \frac{1}{R_{\mathrm{macro0}}}\right). \tag{4}$$

where L and W are the length (9.1 mm) and width (3.8 mm) of the measured surface area and σ_{macro0} (R_{macro0}) is the conductivity (resistance) before the Na deposition. As shown in Fig. 4, the conductivity decreases monotonically and, by the completion of Na adsorption of stage **I**, σ_{macro} has reduced also by ~3 μS/□. It is noted that a number of data points in Fig. 4 are quite different between the two measurements due to different experimental procedures, as described above. Despite the distinctive characters of two independent experimental methods, the measured conductivity changes were consistent with each other. Therefore, it is clear that the surface conductivity reduced several μS/□ by the completion of the Na adsorption of stage **I**. Since the phenomenon is a surface event, the conductivity change can be attributed to the layers near the surface, namely, the superstructure Si(111)7×7 and the space-charge layer. As shown in Fig. 2, bulk bands at the subsurface bended 60 meV toward E_F through the surface transition. Then the associated conductivity change in the space-charge layer is estimated as[2] −3.1 to −1.2 μS for an n-type Si wafer (1–10 Ω cm) and −0.089–−0.15 μS for a p-type Si wafer (3900–6400 Ω cm). Therefore, the conductivity decrease in Figs. 3 and 4 could be explained in terms of a change in space-charge layers for the moderately doped n-type Si wafer but not for the "nondoped" p-type Si wafer. As previously reported and as described in Fig. 2, the stage **I** corresponds to formation of the 2D Na gas on Si(111)7×7 and it induces the metal-to-insulator transition. Therefore, the decrease in the conductivity is due to interruption of the electrical channel of the metallic surface state (S_1). Namely, from the present experiment, we can say that the conductivity of metallic dangling-bond state is ~3 μS at room temperature.

For a comparison, sheet conductivity of the present and previous transport experiments is listed in Fig. 1(b). Conductivities determined by experiments with intact Si(111) samples range from 0.5 to 30 μS and our results also found in the same region. Conductivity measurements on the clean and oxygen-covered Si(111)7×7 surfaces show quite large uncertainty due to entangling nature of surface, bulk, and space-charge-layer conductivity in Si(111)7×7, as described above. On the other hand, the metal-to-insulator transition, induced by very small amount of Na deposition, did not destroy the 7×7 surface structure and it disturbed selectively the channel through the metallic dangling-bond state. As a consequence, the present procedure succeeded in narrowing the range of dc conductivity, 2–4 μS at room temperature, of the Si(111)7×7 surface state.

In Fig. 1(b), sheet conductivity of the Ioffe-Regel (IR) limit for the two-dimensional case is indicated: $\sigma_{\mathrm{IR}} = e^2/h(k_F l) = e^2/h(1) = 39$ μS, where k_F and l are Fermi wave number and carrier mean-free path, respectively. In two dimensions, electron transport is in metallic conduction regime when conductivity is much larger than $\sigma_{\mathrm{IR}} = 39$ μS, while it is in hopping or strong localization regime when it is smaller. Therefore, it seems that the surface-state conductivity of the Si(111)7×7 surface is below the 2D Ioffe-Regel limit and the transport is in strong localization regime. However, the conclusion should be reached after examining the detailed surface band structure of Si(111)7×7.

Concerning the band structure for the dangling-bond state, several types of dispersion curves near the Fermi level have, so far, been reported.[3,4] Photoemission experiments on Si(111)7×7 revealed a single band of free-electron-like type[3] or dressed one.[4] On the other hand, two bands at E_F and one fully occupied band were found from local-density approximation (LDA) calculations of the surface with including correlation effects among electrons in dangling-bond adatom states.[6] The band dispersions along the $\bar{\Gamma}$-$\bar{M}$ line are shown in Fig. 5(a). According to the DAS model, 19 electrons are divided into the dangling-bond state of adatoms, a rest-atom state, and a corner-hole-atom state. The calculations found that bands of rest-atom and corner-hole-atom states were fully occupied by 12 and 2 electrons, respectively, and the dangling-bond bands were filled with remnant five electrons. As shown in Fig. 5(a), one band (1) was fully occupied and two bands (2 and 3) at E_F were partially filled with three electrons, making the Si(111)7×7 surface metallic.[6] On the other hand, it is not easy to understand a relation between a number of surface electrons and a single metallic band. The photoemission researches have also pointed out the issue and proposed possible existence of more than one adatom band near E_F.[3,4]

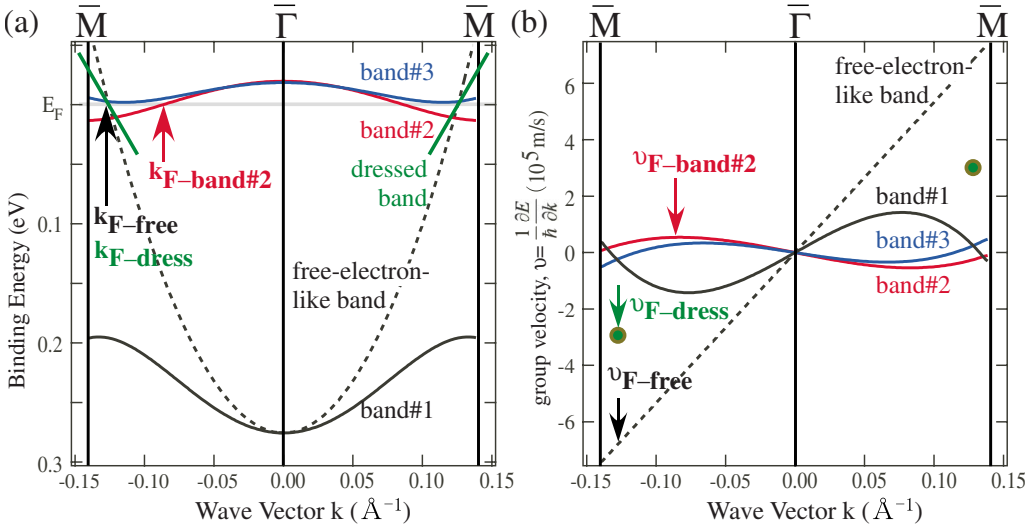

FIG. 5. (Color online) (a) Band dispersion curves of the dangling-bond state of the Si(111)7×7 along the $\bar{\Gamma}$-$\bar{M}$ line (Refs. 3, 4, and 6). A free-electron-like band was reported from photoemission experiment (a broken line) and flat bands (bands 1–3) from a theoretical calculation (solid lines). Dispersion of a dressed band was given by straight (green) lines determined from the reported Fermi vector and Fermi velocity. Fermi wave vectors $k_{F\text{-free}}$, $k_{F\text{-dress}}$, and $k_{F\text{-band 2}}$ are indicated by two arrows. (b) Group velocities v calculated from the bands in (a). Fermi velocities of free-electron-like band, dressed band, and band 2 at the corresponding Fermi vectors are indicated by $v_{F\text{-free}}$, $v_{F\text{-dress}}$, and $v_{F\text{-band 2}}$, respectively.

Let us discuss a relation between the transport property and electronic structure of the Si(111)7×7 surface. The IR limit in Fig. 1(b), which has been used to distinguish between band and hopping conductions in 2D metals, was derived from a free-electron-like band. As shown in Fig. 5(a), some of the reported band dispersions of Si(111)7×7 were non-free-electron-like, indicating breakdown of the Drude model. Therefore, arguments that have been adopted in the previous transport researches, shown in Fig. 1, should be reconsidered. Here, we estimated transport parameters of the cases by the 2D Boltzmann equation and compared with the experimental results. Assuming a constant relaxation time $\tau = \tau(\mathbf{k})$ irrespective of electron wave vector $\mathbf{k}$, the 2D conductivity and Fermi surface are given as follows based on the Boltzmann equation:[14]

$$\sigma_{ij} = \frac{1}{2\pi^2}\frac{e^2\tau}{\hbar}\int \frac{v_{ki}v_{kj}dk_F}{|v_k|}, \tag{5}$$

where k_F and $v_{ki}=(1/\hbar)(\partial E/\partial k_i)$ are the Fermi wave vector and Fermi velocity along $i(=x,y)$ direction, respectively. The integral is done on the Fermi surface. Since some reported band dispersion curves were given along the $\bar{\Gamma}$-$\bar{M}$ line,[3,6] we could only substitute the group velocity along this axis as v_{ki} in Eq. (5) for the comparison. The velocity (v), calculated from the bands in Fig. 5(a), are given in Fig. 5(b). At the Fermi wave number of $k_{F\text{-free}}=0.13$ Å^{-1}, the Fermi velocity $v_{F\text{-free}}$ is $v_{F\text{-free}}=6.7\times10^5$ m/s for the free-electron-like band, while $k_{F\text{-band 2}}=0.23$ Å^{-1} and $v_{F\text{-band 2}}=0.53\times10^5$ m/s for the flat band 2. It is worthy to note that the Fermi wave numbers are defined in the extended-zone scheme. Concerning the dressed band, it was reported $v_{F\text{-dress}}=3\times10^5$ m/s at $k_{F\text{-dress}}=0.13$ Å^{-1}.[4] Using these band parameters and the experimental conductivity, relaxation time and mean-free paths are obtained by inserting them into Eq. (5). For the conductivity values of $\sim3\times10^{-6}$ $\Omega^{-1}\,\square^{-1}$ obtained by the present experiments, relaxation time was 0.9, 6, and 2×10^{-16} s, while the mean-free paths were 0.6, 0.3, and 0.6 Å for band types of free electron, band 2, and dressed, respectively. The obtained paths are much smaller than the size of the 7×7 unit cell (~30 Å) and even than a size of an atom, indicating collapse of the Boltzmann picture.

One can also compare the relaxation time by assuming that τ is determined by electron-phonon interaction since our results were at room temperature, which is higher than surface Debye temperature of Si(111)7×7 (T_D=290 K).[28] Then, τ is given by $\tau\sim\tau_{e\text{-ph}}=\hbar/2\pi\lambda k_BT$ at high-temperature limit ($T>T_D/3$).[25] The dimensionless constant (the mass-enhancement factor) λ represents the strength of the electron-phonon interaction. From the previous temperature-dependent photoemission experiment, λ is λ=1.06 for the Si(111)7×7 surface.[4] Therefore, the relaxation time at T=300 K is $\tau=3.8\times10^{-15}$ s. The relaxation time obtained by the transport measurements through the Boltzmann equation was 1 order of magnitude shorter than the scattering time of electron-phonon interactions. This also indicates failure of a simple picture of metallic band conduction.

These results for transport parameters are similar to the case of Si(557)-Au (Ref. 29) but the previous researches have critical distinctions from the present one. Compared to the defect-rich surface of Si(557)-Au, the Si(111)7×7 surface is almost defect free as directly observed by various microscopies. A lack of impurities of scatterers implies that the system is not simply in hopping conduction or strong localization regime. A combination of a long period of the 7×7 reconstruction (~30 Å) and a surface mean-free path at room temperature (several tens to hundreds of angstroms)[1,25] raises a new intriguing issue in two-dimensional transport phenomena. An effect of electron lo-

calization or quantum interference is likely needed in the consideration. Furthermore, electron correlation effects associated with the dangling-bond states may also play a crucial role in linking between spectroscopy and transport data. It has also been reported that Si(111)7×7 is likely a surface close to a Mott-Hubbard metal-insulator transition.[30,31] Accurate determination of the detailed adatom-state band structure as well as theoretical estimations of the conductance by much sophisticated model such as the Kubo formula is highly requested.

IV. CONCLUSIONS

In summary, we systematically studied electron transport and electronic structure for the metal-to-insulator transition induced by ~0.1 ML Na adsorption on Si(111)7×7 at room temperature. Through measurements during the passivation, conductivity of the metallic dangling-bond state was determined. The value was $(2-4)\times10^{-6}$ $\Omega^{-1}\,\square^{-1}$, which indicated failures of the Drude and Boltzmann models to explain the transport phenomena.

ACKNOWLEDGMENTS

F. Komori and S. Katsumoto are gratefully acknowledged for fruitful discussion. This work was supported by Grants-In-Aid from Japanese Society for the Promotion of Science. M.D. thanks the French Ministry of Foreign Affairs (Bourse Lavoisier) for financial support.

*Present address: Institut des NanoSciences de Paris, Université de Pierre et Marie Curie, UMR 7588 du CNRS, 140 rue de Lourmel, 75015 Paris, France

†imatsuda@issp.u-tokyo.ac.jp

[1] I. Matsuda and S. Hasegawa, J. Phys.: Condens. Matter **19**, 355007 (2007).
[2] S. Hasegawa, X. Tong, S. Takeda, N. Sato, and T. Nagao, Prog. Surf. Sci. **60**, 89 (1999).
[3] R. Losio, K. N. Altmann, and F. J. Himpsel, Phys. Rev. B **61**, 10845 (2000).
[4] I. Barke, F. Zheng, A. R. Konicek, R. C. Hatch, and F. J. Himpsel, Phys. Rev. Lett. **96**, 216801 (2006).
[5] R. I. G. Uhrberg, T. Kaurila, and Y.-C. Chao, Phys. Rev. B **58**, R1730 (1998).
[6] J. Ortega, F. Flores, and A. L. Yeyati, Phys. Rev. B **58**, 4584 (1998).
[7] B. N. J. Persson, Phys. Rev. B **34**, 5916 (1986).
[8] Y. Hasegawa, I.-W. Lyo, and P. Avouris, Surf. Sci. **357**, 32 (1996).
[9] S. Hasegawa and S. Ino, Phys. Rev. Lett. **68**, 1192 (1992).
[10] T. Tanikawa, K. Yoo, I. Matsuda, S. Hasegawa, and Y. Hasegawa, Phys. Rev. B **68**, 113303 (2003).
[11] J. W. Wells, J. F. Kallehauge, T. M. Hansen, and Ph. Hofmann, Phys. Rev. Lett. **97**, 206803 (2006).
[12] K. Yoo and H. H. Weitering, Phys. Rev. B **65**, 115424 (2002).
[13] S. Heike, S. Watanabe, Y. Wada, and T. Hashizume, Phys. Rev. Lett. **81**, 890 (1998).
[14] I. Matsuda, T. Hirahara, M. Konishi, C. Liu, H. Morikawa, M. D'angelo, S. Hasegawa, T. Okuda, and T. Kinoshita, Phys. Rev. B **71**, 235315 (2005).
[15] T. Hirahara, I. Matsuda, C. Liu, R. Hobara, S. Yoshimoto, and S. Hasegawa, Phys. Rev. B **73**, 235332 (2006).
[16] C. L. Petersen, F. Grey, and M. Aono, Surf. Sci. **377**, 676 (1997).
[17] G. Hollinger and F. J. Himpsel, J. Vac. Sci. Technol. A **1**, 640 (1983).
[18] K. Wu, Y. Fujikawa, T. Nagao, Y. Hasegawa, K. S. Nakayama, Q. K. Xue, E. G. Wang, T. Briere, V. Kumar, Y. Kawazoe, S. B. Zhang, and T. Sakurai, Phys. Rev. Lett. **91**, 126101 (2003).
[19] J. R. Ahn, G. J. Yoo, J. T. Seo, J. H. Byun, and H. W. Yeom, Phys. Rev. B **72**, 113309 (2005).
[20] J. J. Paggel, G. Neuhold, H. Haak, and K. Horn, Surf. Sci. **414**, 221 (1998).
[21] M. D'angelo, M. Konishi, I. Matsuda, C. Liu, S. Hasegawa, T. Okuda, and T. Kinoshita, Surf. Sci. **590**, 162 (2005).
[22] H.-J. Neff, I. Matsuda, M. Hengsberger, F. Baumberger, T. Greber, and J. Osterwalder, Phys. Rev. B **64**, 235415 (2001).
[23] A. Zangwill, *Physics at Surfaces* (Cambridge University Press, Cambridge, England, 1988).
[24] T. Tanikawa, I. Matsuda, T. Kanagawa, and S. Hasegawa, Phys. Rev. Lett. **93**, 016801 (2004).
[25] I. Matsuda, C. Liu, T. Hirahara, M. Ueno, T. Tanikawa, T. Kanagawa, R. Hobara, S. Yamazaki, S. Hasegawa, and K. Kobayashi, Phys. Rev. Lett. **99**, 146805 (2007).
[26] I. Matsuda, M. Ueno, T. Hirahara, R. Hobara, H. Morikawa, C. Liu, and S. Hasegawa, Phys. Rev. Lett. **93**, 236801 (2004).
[27] H. Okino, I. Matsuda, S. Yamazaki, R. Hobara, and S. Hasegawa, Phys. Rev. B **76**, 035424 (2007).
[28] Y. Fukaya, A. Kawasuso, K. Hayashi, and A. Ichimiya, Phys. Rev. B **70**, 245422 (2004).
[29] H. Okino, R. Hobara, I. Matsuda, T. Kanagawa, S. Hasegawa, J. Okabayashi, S. Toyoda, M. Oshima, and K. Ono, Phys. Rev. B **70**, 113404 (2004).
[30] D. Fick, C. Bromberger, H. J. Jansch, O. Kuhlert, R. Schillinger, and C. Weindel, Surf. Sci. **600**, 3835 (2006).
[31] R. Schillinger, C. Bromberger, H. J. Jansch, H. Kleine, O. Kuhlert, C. Weindel, and D. Fick, Phys. Rev. B **72**, 115314 (2005).